A Novel Molecular Imprint Polymer Synthesis for Solid Phase Extraction of Andrographolide

Hemavathi Krishnan[1,*], A.K.M. Shafiqul Islam[1,2], Zainab Hamzah[1], Pubalan Nadaraja[3], and Mohd Noor Ahmad[4]

[1]*Department of Chemical Engineering Technology, Universiti Malaysia Perlis, Uniciti Alam Campus, Sungai Chuchuh, 02100 Padang Besar, Perlis, Malaysia*

[2]*School of Chemical Sciences, Universiti Sains Malaysia, 11800 Minden, Pulau Pinang, Malaysia*

[3]*Centre of Diploma Studies, Universiti Malaysia Perlis, Uniciti Alam Campus, Sungai Chuchuh, 02100 Padang Besar, Perlis, Malaysia*

[4]*Department of Electrical and Electronics, British Malaysian Institute, Universiti Kuala Lumpur, 53100 Gombak, Selangor, Malaysia*

* ***Corresponding author:***

tel: +6016-6344362
email: hemavathi.krishnan@gmail.com

Received: March 28, 2018
Accepted: September 20, 2018

DOI: 10.22146/ijc.34369

Abstract: *The use of molecularly imprinted polymers for solid phase micro-extraction (SPME) of bioactive compounds are getting popularity. The interest on efficient extraction process of andrographolide from the plant is increasing due to their vast therapeutic applications. In this study, andrographolide imprinted MIP was prepared by precipitation polymerization method using the non-covalent technique to use as sorbent materials for solid phase extraction of the bioactive compound. HyperChem 8.0.10 software was used to investigate and optimize the template and functional monomer ratio in the pre-polymerization system to synthesize the imprinted polymers. Molecular modeling gives information about molecular interactions and the Gibbs free energies of the pre-polymerization complex. Based on the computational study, andrographolide, methacrylic acid (MAA) and ethylene glycol dimethacrylate (EGDMA) were used as the template, functional monomer, and cross-linker, respectively at the 1:3:20 ratios. The MIPs were characterized by kinetic study and imprinting factor. The binding parameters for the recognition of andrographolide were studied using Langmuir, Freundlich and Langmuir-Freundlich adsorption isotherm models. Andrographolide MIP contains the maximum number of binding sites with the adsorption capacity of 149.59 μg/g. The SPME experimental data best fit with Langmuir-Freundlich isotherm model with the R2 value of 0.997. This research shows that the MIPs prepared by precipitation polymerization gives a good extraction capability using SPME method.*

Keywords: *andrographolide; molecularly imprinted polymer; precipitation polymerization; adsorption isotherm*

■ INTRODUCTION

Andrographis paniculata is a popular medicinal plant locally known as "Hempedu Bumi" in Malaysia. *A. paniculata* extracts are widely used in China, India, Thailand and other Southeast Asian countries [1] which exerted varieties of medicinal effects, including anti-inflammatory [2-3], anticancer [4] and anti-oxidative [5]. A number of bioactive compounds are reported from the plant, which mainly includes diterpenoid lactones, flavonoids and polyphenols [6]. Andrographolide (Fig. 1) is among the most promising bioactive diterpenoid lactone in *A. paniculata,* which mainly contained in the leaves [7]. Recently researchers

reported andrographolide to have activity against a number of viruses, including human immunodeficiency virus (HIV) [8], hepatitis B [9], influenza [10], hepatoma cancer cells [11] and hepatitis C [12].

There is growing interest to efficiently extract andrographolide from the plant due to its vast therapeutic applications [13-15]. Solid phase extraction, liquid-liquid extraction, and ultrafiltration are the commonly used separation techniques to isolate andrographolide. However, these methods are commonly used for sample pre-treatment, and their selectivity is poor. The use of molecularly imprinted polymers as sorbent material is a promising technology for the bioactive extraction and purification [16]. Recently researches are using molecular imprint polymer technique to selectively extract the target compounds from herbal plants.

Molecular imprinting is a rapidly emerging technology to synthesize polymers having specific molecular recognition properties of a target compound [17]. It consists of synthetic macromolecular matrixes which give a pre-arranged polymeric nanostructured materials by forming specific hollow cavities similar to the template morphology [18]. Molecularly imprinted polymers are synthesized by mixing the template molecule with functional monomers, cross-linking monomers and a radical initiator in aprotic porogen. The removal of the template from the polymer matrix leaves cavities that are complementary to the template molecules and possess specific rebinding capabilities [19].

The success of molecular imprinting generally depends on the choice of the functional monomer used in the synthesis of molecularly imprinted polymer (MIP). Before polymerization, the level of interaction between the template and the functional monomer is an important factor to be considered to develop the effective MIP with good affinity. MIP synthesis is typically a quiet time-consuming process which often requires experimental practices through the variation of functional monomers and solvents. Conventionally, selecting optimal imprinting conditions are based on the trial and error approach, which is a tedious method [20]. A better method and understanding on the mechanism of molecular imprinting process is a rationally computational design.

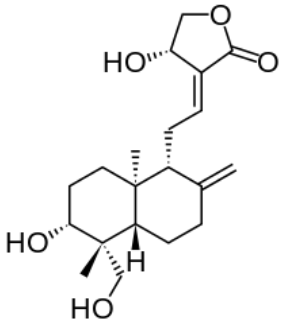

Fig 1. Molecular structure of Andrographolide

MIPs are synthesized in various forms such as porous microspheres, thin films, bulk monoliths, and hydrogels. MIPs as solid sorbents with pre-determined molecular selectivity have shown as an attractive solution for efficient extraction [21]. To use MIPs as a sorbent for solid phase micro-extraction (SPME) application, it requires monodispersed and micro-spherical particles. Several polymerization methods have been developed to prepare spherical and uniform MIPs, such as emulsion polymerization, multi-step swelling polymerization, and suspension polymerization. But these method associated with some complications, such as complex procedures, special stabilizers, and surfactants requirement, which is hard to remove from MIPs [21]. Precipitation polymerization is a promising technique for the synthesis of polymers in the form of porous beads [21]. The globular polymer morphology from this technique eases the extraction process and improves the performance of MIPs. The objective of this present research was to optimize the binding sites distribution of the synthesized MIP by using adsorption isotherm studies. The corresponding results were validated by synthesis of MIP using precipitation polymerization and applying SPME.

■ EXPERIMENTAL SECTION

Materials and Instrumentation

Andrographolide (98%), methacrylic acid (MAA), ethylene glycol dimethacrylate (EGDMA) and 2,2'-azobisisobutyronitrile (AIBN) were purchased from Aldrich Chem. Co. (Milwaukee, WI, USA). All the solvents used including acetonitrile, toluene, glacial acetic acid, and methanol were analytical grade and

purchased from Merck AG. The centrifuge was used to sediment MIP precipitates, solid phase micro extractor (Supelco) was used to perform the rebinding assay and UV-Vis spectrophotometer (Perkin-Elmer) was used to determine the initial and equilibrium concentration.

Computational Design of MIP

The HyperChem 8.0.10 (Hypercube Inc.) software was used in this work. Acrylamide (AAM), Acrylic acid (AA), Methacrylic acid (MAA), Itaconic acid (IA) and Hydroxyethyl methacrylate (HEMA) were used as a functional monomer for computational design of MIP. Initially, 3D molecular models of the template and functional monomers were built and the coordinates of stable conformers were generated to prepare input file for running molecular modeling simulation. Possible conformations of the template and functional monomer as 1:n (n < 4) were designed and simulated to geometrically optimize the complex at the lowest energy level in the vacuum phase [22]. Complex formation abilities of AAM, AA, MAA, IA, and HEMA with template molecule were theoretically compared by applying a Restricted Hartree-Fock (RHF) semi-empirical method based on molecular orbital theory. The structures of the template and functional monomer complex molecules were optimized using the PM3 method at ground state by minimizing the binding energy of the molecules. The conjugate gradients process (Polak-Ribier) was used for the geometry optimization using a convergence set at the value of 0.01 Kcal/(Å.mol). During energy minimization, the simulation searches for a molecular structure in which the little changes of geometry to give the most stable configuration. Gibbs free binding energy difference (ΔE) during the complex formation was calculated with Equation (1) [23]. The modeling helps to explore the effect of the non-covalent interactions, specifically the hydrogen bond (H-bond) in growing polymer chain during polymerization of stable template – functional monomer complexation.

$$\Delta E = E_{(\text{template–monomer complex})} - \left[E_{\text{template}} + n\left(E_{\text{monomer}}\right) \right] \quad (1)$$

where, $\Delta E_{(\text{template-monomer complex})}$ = non-covalent binding energy of template monomer complex; $\Delta E_{(\text{template})}$ = binding energy of template; $\Sigma E_{(\text{monomer})}$ = Energy of monomer ratio (n = 1, 2, 3, 4)

Synthesis of molecularly imprinted polymer

The MIP was synthesized by precipitation polymerization technique. Andrographolide (template) (0.3 mmol) and MAA (0.9 mmol) were dissolved in 50 mL of acetonitrile/toluene (3:1 v/v). The reaction mixture was sonicated for 5 min. EGDMA of 6.0 mmol and AIBN (20 mg) were added respectively into the mixture and nitrogen gas purged for 20 min. The final reaction mixture was sealed and allowed to stir at 60 °C for 24 h. When the precipitation polymerization process was completed, the polymers were sedimented by centrifuge at 10,000 rpm. Subsequently, the polymers were washed with methanol/acetic acid (90:10 v/v) mixture several times until the template molecules were completely removed. Finally, MIPs were washed three times with each of methanol and distilled water to remove acid and dried under vacuum oven. Non-imprinted polymers (NIPs) were prepared in the same manner excluding the addition of *the* template molecule. The MIP synthesis process is shown in Fig. 2.

Kinetic study and imprinting factor

One hundred mg of MIPs and NIPs were placed into 30 mL vials. Each vial was loaded with 25 mL of 0.025 mg/L (C_i) andrographolide solution. The mixtures were stirred in thermo-mixer at 100 rpm for 10 h. Two mL of the sample taken from the mixture for every 2 h and filtered using Nylon (0.2 μm) syringe filters. The absorbance of the final liquid was measured at 225 nm using UV-VIS spectrophotometer to determine the remaining concentration (C_e) of the template in the solution [24]. Imprinting factor was calculated to compare the imprinting effect of MIPs and NIPs.

MIP-SPME procedure

A polyethylene frit (20 μm porosity) was placed at the bottom of each 1mL SPME cartridges. One hundred mg of MIPs and NIPs were packed into the cartridges and another frit was placed on the top of the cartridges. Subsequently, the pack was conditioned twice with deionized water and once with methanol. Five mL of

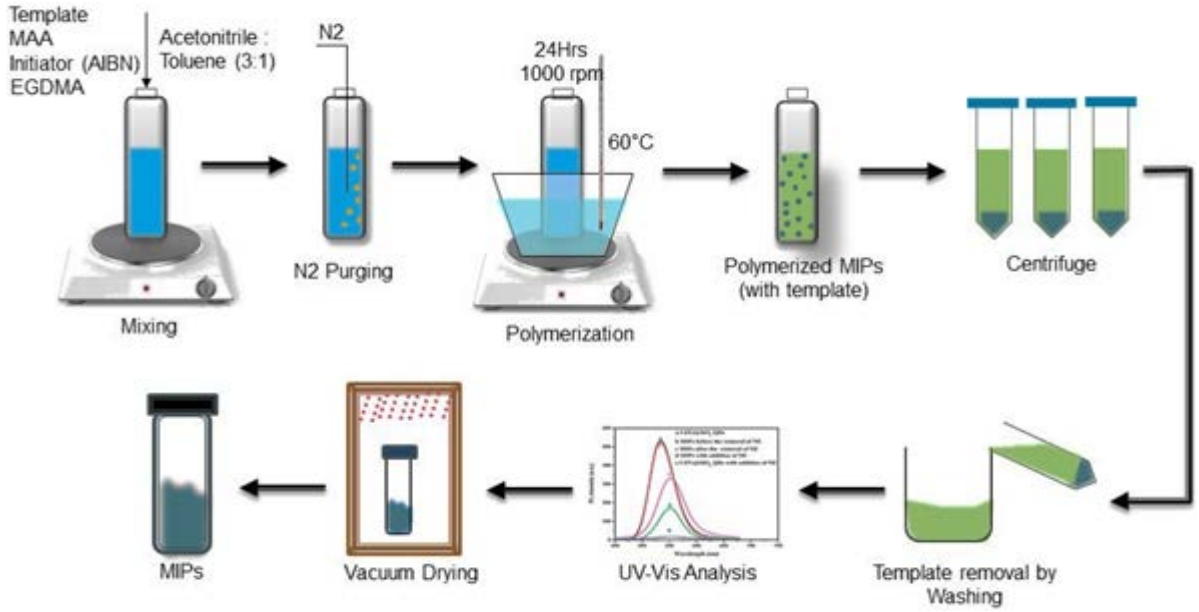

Fig 2. Synthesis of andrographolide imprinted polymer by precipitation polymerization

template solutions with different concentrations were forced to pass through the system by regulating the vacuum at 20 KPa. The eluates were collected for UV spectrophotometer analysis to determine the remaining template concentration.

Adsorption Isotherm

The equilibrium adsorption capacity (Q_e, mg/g) was calculated according to the following equation:

$$Q_e = (C_i - C_e) X \frac{v}{m} \quad (2)$$

where, C_i and C_e are initial and equilibrium concentrations (mmol/L), respectively, V is the volume of sample solution (L) and m is the mass of Sorbent (g) [25]. The adsorption data were fitted into Langmuir, Freundlich and Langmuir-Freundlich Isotherm models [26].

$$Q_e = \frac{Q_{max} b C_e}{1 + b C_e} \quad (3)$$

$$Q_e = K_F C_e^{1/n} \quad (4)$$

$$Q_e = \frac{Q_{max} \cdot (b C_e)^{1/n}}{1 + (b C_e)^{1/n}} \quad (5)$$

where Q_{max} is maximum saturation capacity (mg/g). b is the equilibrium constant (L/mg), a high value indicates a steep beginning of the isotherm and the higher affinity of the adsorbent for the absorbate, K_F is the Freundlich equation constant (mg/g)(L/mg)$^{1/n}$ which is related to the adsorption capacity and n is empirical parameter which varies with heterogeneity, the value greater than 1 indicates higher heterogeneity [26]. The best-fitted model was calculated according to the minimum residual sum of squares value. The parameters were calculated by non-linear regression using Microsoft Excel Solver function.

■ RESULTS AND DISCUSSION

MIP Design by Computational Approach

During simulation and molecular modeling study, the interaction between the template and functional monomers were studied which involves both covalent bonding and one or more intermolecular attraction via noncovalent bonding. These interactions can exist as hydrogen bonding, van der Waals interaction or only London force. The comparison of the binding energies of each template-monomer complex helps to decide the degree of bonding level and the interaction type. The highest complex energy ($E_{complex}$) was chosen for every ratio to estimate and calculate the binding energy difference between template and functional monomer. However, the average energy of hydrogen bonds was required to get the stable complex.

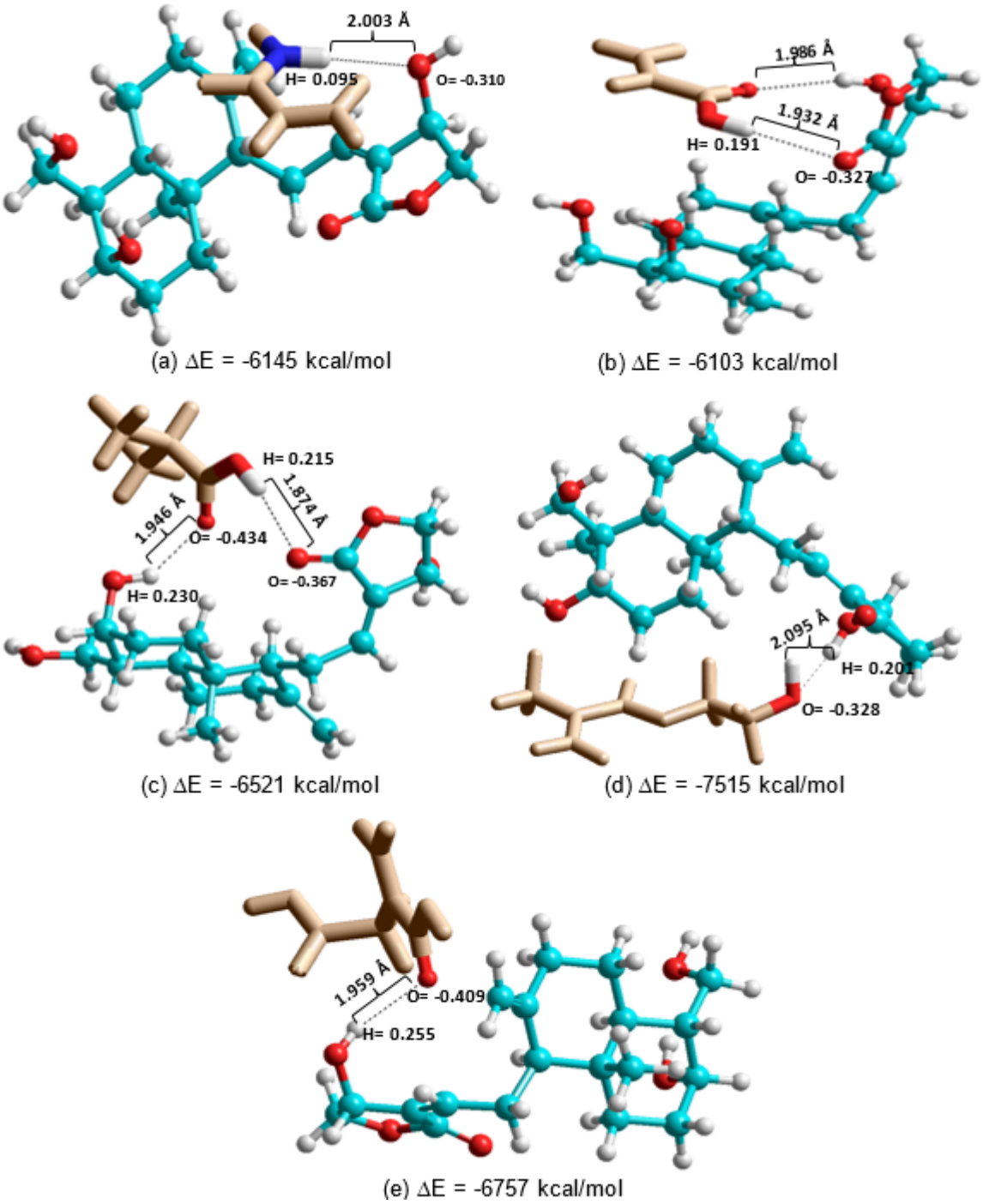

Fig 3. Optimized structures of pre-polymerization complex at 1:1 ratio. (a) andrographolide: acrylamide, (b) andrographolide : acrylic acid, (c) andrographolide : methacrylic acid, (d) andrographolide : hydroxy ethyl methacrylate, and (e) andrographolide : itaconic acid

The template-monomer complexes were analyzed to determine the nature of the interaction between the functional monomer and andrographolide. Every stable and optimum template-monomer complex for each monomer and their geometrical parameters such as bond length, angle, and charges are as shown in Fig. 3. HyperChem 8.0.10 creates a hydrogen bond if the distance between the donor hydrogen and acceptor

atom is less than 3.2 Å and the angle made by the covalent bonds to the donor and acceptor atoms is greater than 150 degrees [27]. Pardeshi et al. [28] and Liang et al. [29] used a computational approach to screen monomers using the binding energy of the template and monomers as a measure of their interaction. Nezhadali et al. [30] used the similar approach to select the best functional monomer for the template 1,4-dihydroxyanthraquinone to develop a sensor.

In this study, MAA formed a stable complex with the template as it is a bidentate ligand which is able to donate and accept electrons at two functional groups at the same time. As shown in Fig. 3(c), the O of andrographolide which has strong electron source (-0.367e) and the H of MAA which has large positive charge (+0.215e) were attracted to form a hydrogen bond. Similarly, in Fig. 3(e) where H of andrographolide has large positive charge (+0.255e) and the O of itaconic acid has electron source (-0.409e). The more electronegative the atom attracted to H, the stronger the bond. The carboxylic functional groups of acidic functional monomers is an excellent hydrogen bond donor and acceptor which can participate in the formation of hydrogen bonding interactions with the template. Due to this property, acidic functional monomers were used for imprinting of organic template molecules.

In the case of methacrylic acid, acrylic acid, hydroxyethyl methacrylate and itaconic acid, the carboxylic group (-COOH) functional group interacted with andrographolide. The interaction of acrylamide was observed between the amine ($-NH_2$) functional group and C=O of the template. The H-bonding distance for AND-AA was found to be 1.93 Å and it was the shortest among all the complex. The bond distance for most of the complexes is in the range of 1.8–2.0 Å, which proves the formation of hydrogen bond [31]. The hydrogen bonds are formed between proton donors such as N-H and O-H and proton acceptors such as C=O. The hydrogen bond formed due to shifting of a proton to another electronegative atom. It was also observed that, as the bond distance increased, the value of binding energy (ΔE) decreased.

Table 1. Gibbs free energy changes (ΔE) due to the complex formation between the template and the functional monomers

Template-monomer complex	ΔE (kcal/mol)
Andrographolide – Acrylamide	-218.95
Andrographolide – Acrylic acid	-108.53
Andrographolide – Methacrylic acid	-284.58
Andrographolide – Itaconic acid	-270.92
Andrographolide – Hydroxyethyl methacrylate	-177.17

The binding energy of the template-functional monomer complex at 1:1 ratio are presented in Table 1. The interaction energies obtained by docking the template and the monomer structures. Gibbs free energy changes were calculated using equation 1. MAA and IA obtained the lowest energy among other functional monomers. Therefore, it is concluded that they possess the strongest affinity for andrographolide.

Optimization of Template-Monomer Complex Ratio

In the computational study, the template and functional monomers are simulated from 1:1 to 1:4 ratio to screen the suitable amount for complex formation. Mole ratio optimization of the template-monomer complex was carried out to test the influence of excess functional monomer concentration. The selection of the functional monomer and the ratio is based on binding energy calculation according to equation (1) which are within the range of non-covalent interactions. According to Mancin [31], the energy ranges between 2–30 kcal/mol defines the non-covalent interaction and falls in the hydrogen bond category.

The Gibbs free binding energy (ΔE) of template-monomer complexes with a different mole ratio of functional monomer are shown in Fig. 4. The binding energy between template and MAA was 24.27 kcal/mol at a mole ratio of 1:3 and the binding energy between the template and IA was 30.55 kcal/mol was at 1:2. Pardeshi et al. [28] obtained the similar range of binding energies in their computational study of gallic acid as a template with 15 types of functional monomers. According to

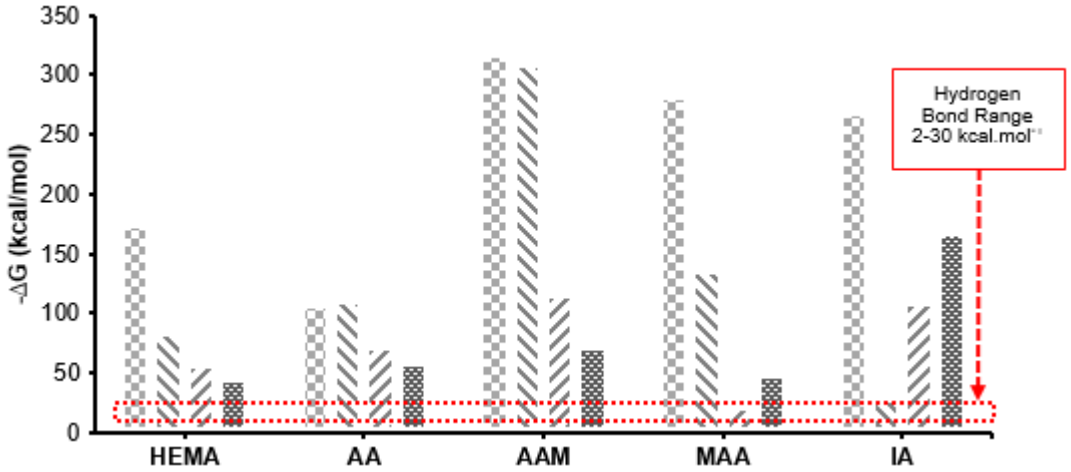

Fig 4. The ΔE value of template-monomer complexes in different mole ratios. = 1:1, = 1:2, 1:3 and = 1:4

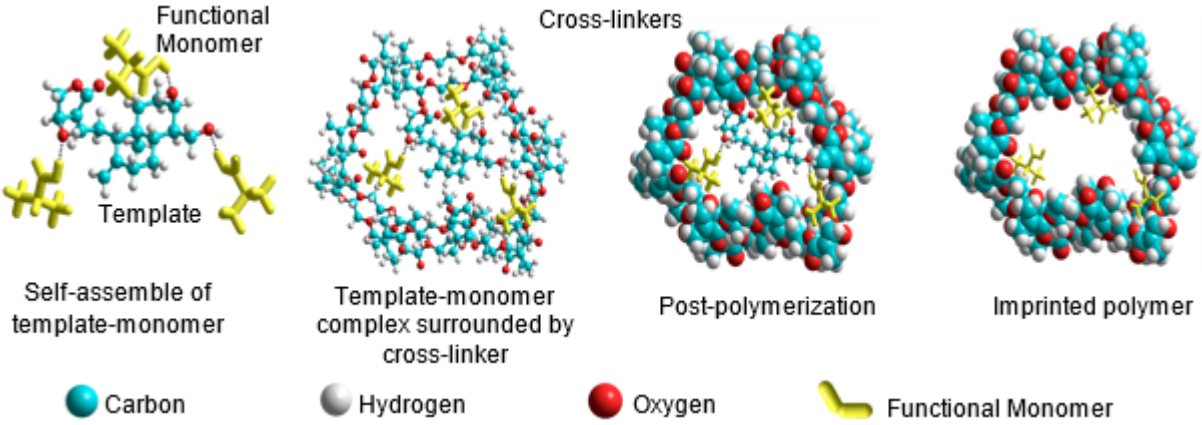

Fig 5. Andrographolide imprinted polymer synthesis method in molecular level

Mancin [31], both MAA and IA falls in the range of non-covalent hydrogen bonding. Andrographolide-MAA possesses the lowest energy by holding three functional monomers where andrographolide-IA was only able to bind only two functional monomers. Therefore, MAA was chosen as a strongest functional monomer at an optimum ratio of 1:3. Khan et al. [32] also selected MAA as copolymer to imprint benzo-α-pyrene-based on computational approach.

MIP Synthesis

The non-covalent approach was used to synthesize MIP. MAA was selected as a functional monomer due to its Hydrogen donor and acceptor capability to diterpene lactone template molecule.

In andrographolide molecule, there are three hydroxyl groups (O-H) and one carbonyl group (C=O). The carboxylic group (-COOH) of MAA interacted with proton donors such as O-H, and proton acceptors such as C=O. These combinations have been frozen by adding EGDMA to give rigid structures. The specific imprinting sites were preserved after removal of the template molecule. These cavities with binding sites were able to selectively adsorb andrographolide molecule. The MIP synthesis process in molecular level is shown in Fig. 5.

Kinetic Study and Imprinting Factor

The adsorption capacities Q of MIP and NIP toward andrographolide were calculated using equation (2). The different between adsorption capacities show that MIP is more selective towards andrographolide. Polymer prepared with andrographolide as a template contains cavity sites that are a compliment to andrographolide. Those cavities rapidly adsorbed the

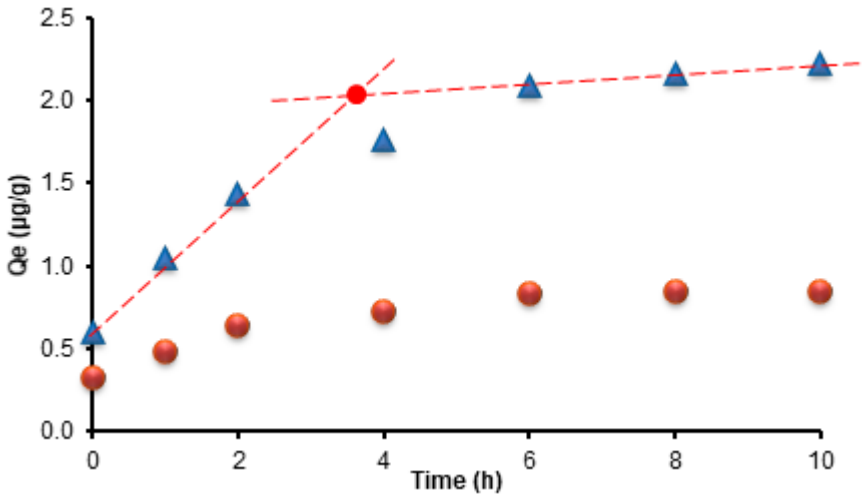

Fig 6. Adsorption dynamic curves of andrographolide on to the polymers (▲ MIP and ● NIP)

template molecule when coming in contact.

Adsorption capability of MIP and NIP were analyzed at every two hours as shown in Fig. 6. For the first two hours, the adsorption rate is rapid, while the next four hours, the adsorption rate was slowed down. This happened due to the occupation of template molecules in the MIP hollow space. The saturated point X was observed at 3rd hour. Once all the binding sites are fully occupied, there was no adsorption observed after 8 h. Although NIPs showing a similar trend with MIPs, the amount of andrographolide bound is lower than MIP due to its non-specific binding sites. Additionally, NIPs did not reach a saturation point as the non-specific binding sites attach and detach template molecules on the functional groups present in functional monomer or cross-linkers.

The effectiveness of prepared polymer is evaluated using imprinting factor (IF) and cavities distribution ratio (K_d). The distribution ratio (K_d) of cavities was calculated using,

$$K_d = \frac{(C_i - C_e)v}{(C_e) * m} \quad (6)$$

where, C_i = 0.025 µg/mL (initial concentration), C_e = final concentration obtained from standard curve, v = 25 mL of stock solution and m = 100 mg of MIP/NIP. The distribution cavities are influenced by the type of monomer, cross-linker, and porogen. The cavities distribution for MIP and NIP is 55.45 and 24.53 mL/g, respectively. From the data, it is concluded that the imprinted cavities of MIPs cause the high binding affinity to the template molecule in the polymer matrix. The cavities distribution, K_d is higher in MIP which leads to more affinity to the template. Based on the cavities distribution ratio, the IF of MIP is 2.26. The IF value is an assessment of ratio, between the numbers of specific interactions, (C_i) to the number of non-specific interactions, (C_e).

Adsorption Binding Isotherm

Solid phase microextraction was used to test the binding assay of MIP. There are four steps in SPME usage i.e. conditioning, sample loading, washing, and elution. MIP and NIP were packed as the stationary phase in between frits and it was conditioned with deionized water. The sample solutions with different concentrations were forced to pass through the system by regulating the vacuum at 20 KPa. Finally, the eluates were collected for analysis with UV-Vis spectrophotometer. Fig. 7(a) shows the andrographolide adsorption capacity of MIPs and NIPs, where Q is the amount of andrographolide adsorbed at the elevating concentration. The adsorption capacity of MIP increased quickly with the increase in concentration. The curve trends in each isotherm indicate the existence of equilibrium point in both MIPs and NIPs. The curve trend shows that the MIP contains no more binding sites

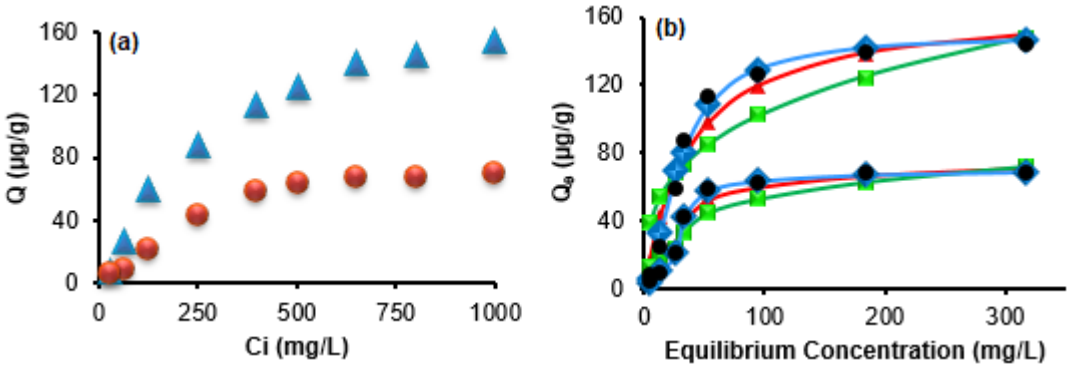

Fig 7. Adsorption isotherm of MIP and NIP. (a) experimental data and (b) adsorption isotherm fitting curve. ● Experimental, ▲ Langmuir, ■ Freundlich, ◆ Langmuir-Freundlich

Table 2. Fitting parameters of adsorption isotherms of MIP and NIP by non-linear regression

Fitting Parameters	Langmuir (L)		Freundlich (F)		Langmuir-Freundlich (L-F)	
	MIP	NIP	MIP	NIP	MIP	NIP
Q_{max} (mg/g)	167.86	88.47	-	-	149.588	71.530
b $(mg/g)(L/mg)^{1/n}$	0.026	0.007			1.587	1.749
K_F (L/mg)			24.905	3.705		
n	-	-	0.466	0.309	0.005	0.004
R^2	0.961	0.977	0.820	0.897	0.997	0.899
ΣRSS	902.36	203.69	460.87	910.37	90.69	10.44

when all the cavities are occupied by templates and saturated. Although NIPs show similar trends with MIPs, they possess the lower adsorption capacity and lower saturation point. This is because of non-specific recognition sites in the non-imprinted polymer. Two different Q values of MIP and NIP at elevated concentration shows the presence of complementary cavities to andrographolide in MIP.

The experimental data were fitted into three isotherm models i.e. Langmuir, Freundlich, and Langmuir-Freundlich using Microsoft Excel Solver function. Fig. 7(b) shows a non-linear curve for Langmuir (L), Freundlich (F) and Langmuir-Freundlich (LF) isotherm for MIP and NIP. The trend shows that the experimental data follows Langmuir-Freundlich isotherm. This model describes the relationship between the saturation concentration of Q_e and free template molecules at the equilibrium point (C_e).

Generally, MIPs contains the highest number of binding sites (Q_{max}) compared to NIPs. This is proven by isotherm parameters as shown in Table 2. The theoretical values of Q_{max} of MIP and NIP according to Langmuir isotherm were calculated and found 167.86 and 88.47 µg/g, respectively. Whereas, the theoretical values of Q_{max} of MIP and NIP according to Langmuir-Freundlich isotherm was found to be 149.59 and 71.53 µg/g. According to minimum ΣRSS value and R^2 value, MIPs well suited with Langmuir-Freundlich isotherm model. The lower heterogeneity parameter, n close to zero indicates the existence of homogeneous binding site distribution. The observed trend can be attributed to the adsorption of andrographolide on to the MIP polymers.

■ CONCLUSION

In recent years, SPME became an efficient method in separation technology, especially for bioactive compounds. This work presents a new SPME sorbent for the selective isolation of andrographolide. The template and monomer ratio was optimized in the pre-polymerization system using computational quantum chemical approach. MAA was selected as a best functional monomer to synthesize andrographolide

imprinted polymer at a 1:3 ratio. Andrographolide imprinted polymer was prepared by precipitation polymerization using MAA and EGDMA as functional monomer and cross-linker, respectively. Adsorption isotherm of andrographolide MIP reveals that it has followed Langmuir-Freundlich isotherm which has distributed specific binding sites. The andrographolide imprinted polymer shows MIP high extraction efficient sorbent material results with imprinting factor of 2.26.

■ ACKNOWLEDGMENTS

Authors gratefully acknowledge the Ministry of Higher Education, Malaysia for financial support by fundamental research grant No. KPT-FRGS 9003-00406.

■ REFERENCES

[1] Thakur, A.K., Chatterjee, S.S., and Kumar, V., 2015, Adaptogenic potential of andrographolide: An active principle of the king of bitters (*Andrographis paniculata*), *J. Tradit. Complement. Med.*, 5 (1), 42–50.

[2] Wen, L., Xia, N., Chen, X., Li, Y., Hong, Y., Liu, Y., Wang, Z., and Liu, Y., 2014, Activity of antibacterial, antiviral, anti-inflammatory in compounds andrographolide salt, *Eur. J. Pharmacol.*, 740, 421–427.

[3] Okhuarobo, A., Falodun, J.E., Erharuyi, O., Imieje, V., Falodun, A., and Langer, P., 2014, Harnessing the medicinal properties of *Andrographis paniculata* for diseases and beyond: A review of its phytochemistry and pharmacology, *Asian Pac. J. Trop. Dis.*, 4 (3), 213–222.

[4] Jada, S.R., Subur, G.S., Matthews, C., Hamzah, A.S., Lajis, N.H., Saad, M.S., Stevens, M.F.G., and Stanslas, J., 2007, Semisynthesis and *in vitro* anticancer activities of andrographolide analogues, *Phytochemistry*, 68 (6), 904–912.

[5] Pandeti, S., Sonkar, R., Shukla, A., Bhatia, G., and Tadigoppula, N., 2013, Synthesis of new andrographolide derivatives and evaluation of their antidyslipidemic, LDL-oxidation and antioxidant activity, *Eur. J. Med. Chem.*, 69, 439–448.

[6] Rao, Y.K., Vimalamma, G., Rao, C.V., and Tzeng, Y.M., 2004, Flavonoids and andrographolides from *Andrographis paniculata*, *Phytochemistry*, 65 (16), 2317–2321.

[7] Song, Y.X., Liu, S.P., Jin, Z., Qin, J.F., and Jiang, Z.Y., 2013, Qualitative and quantitative analysis of *Andrographis paniculata* by rapid resolution liquid chromatography/time-of-flight mass spectrometry, *Molecules*, 18 (10), 12192–12207.

[8] Wang, B., Li, J., Huang, W.L., Zhang, H.B., Qian, H., and Zheng, Y.T., 2011, Synthesis and biological evaluation of andrographolide derivatives as potent anti-HIV agents, *Chin. Chem. Lett.*, 22 (7), 781–784.

[9] Chen, H., Ma, Y.B., Huang, X.Y., Geng, C.A., Zhao, Y., Wang, L.J., Guo, R.H., Liang, W.J., Zhang, X.M., and Chen, J.J., 2014, Synthesis, structure-activity relationships and biological evaluation of dehydroandrographolide and andrographolide derivatives as novel anti-hepatitis B virus agents, *Bioorg. Med. Chem. Lett.*, 24 (10), 2353–2359.

[10] Seniya, C., Shrivastava, S., Singh, S., and Khan, G.J., 2014, Analyzing the interaction of a herbal compound Andrographolide from *Andrographis paniculata* as a folklore against swine flu (H1N1), *Asian Pac. J. Trop. Dis.*, 4 (Suppl. 2), S624–S630.

[11] Ji, L., Zheng, Z., Shi, L., Huang, Y., Lu, B., and Wang, Z., 2015, Andrographolide decreased VEGFD expression in hepatoma cancer cells by inducing ubiquitin/proteasome-mediated cFos protein degradation, *Biochim. Biophys. Acta, Gen. Subj.*, 1850 (4), 750–758.

[12] Hafid, A.F., Utsubo, C.A., Permanasari, A.A., Adianti, M., Tumewu, L., Widyawaruyanti, A., Wahyuningsih, S.P.A., Wahyuni, T.S., Lusida, M.I., Soetjipto., and Hotta, H., 2017, Antiviral activity of the dichloromethane extracts from *Artocarpus heterophyllus* leaves against hepatitis C virus, *Asian Pac. J. Trop. Biomed.*, 7 (7), 633–639.

[13] Wongkittipong, R., Prat, L., Damronglerd, S., and Gourdon, C., 2004, Solid-liquid extraction of andrographolide from plants - Experimental study, kinetic reaction and model, *Sep. Purif. Technol.*, 40 (2), 147–154.

[14] Majee, C., Gupta, B.K., Mazumder, R., and Chakraborthy, G.S., 2011, HPLC method

development and characterization of bio-active molecule isolated from *Andrographis paniculata*, *Int. J. PharmTech Res.*, 3 (3), 1586–1592.

[15] Kumar, S., Dhanani, T., and Shah, S., 2014, Extraction of three bioactive diterpenoids from *Andrographis paniculata*: Effect of the extraction techniques on extract composition and quantification of three andrographolides using high-performance liquid chromatography, *J. Chromatogr. Sci.*, 52 (9), 1043–50.

[16] Ahmadi, F., Yawari, E., and Nikbakht, M., 2014, Computational design of an enantioselective molecular imprinted polymer for the solid phase extraction of S-warfarin from plasma, *J. Chromatogr. A*, 1338, 9–16.

[17] Islam, A.K.M.S., Krishnan, H., Singh, H., and Ahmad, M.N., 2015, A noble molecular imprint polymer biosensor for caffeic acid detection in orthosiphon Stamineus extracts, *Jurnal Teknologi*, 77 (7), 97–101.

[18] Krishnan, H., Islam, A.K.M.S., Hamzah, Z., and Ahmad, M.N., 2017, Rational computational design for the development of Andrographolide molecularly imprinted polymer, *AIP Conf. Proc.*, 1891 (1), 020083.

[19] Nicholls, I.A., Andersson, H.S., Golker, K., Henschel, H., Karlsson, B.C.G., Olsson, G.D., Rosengren, A.M., Shoravi, S., Suriyanarayanan, S., Wiklander, J.G., and Wikman, S., 2011, Rational design of biomimetic molecularly imprinted materials: Theoretical and computational strategies for guiding nanoscale structured polymer development, *Anal. Bioanal. Chem.*, 400 (6), 1771–1786.

[20] Pardeshi, S., Dhodapkar, R., and Kumar, A., 2014, Molecularly imprinted microspheres and nanoparticles prepared using precipitation polymerisation method for selective extraction of gallic acid from *Emblica officinalis*, *Food Chem.*, 146, 385–393.

[21] Pardeshi, S., and Singh, S. K., 2016, Precipitation polymerization: a versatile tool for preparing molecularly imprinted polymer beads for chromatography applications, *RSC Adv.*, 6 (28), 23525–23536.

[22] Tahir, I., Ahmad, M.N., Islam, A.K.M.S., and Arbain, D., 2012, Virtual searching of dummy template for Sinensetin based on 2D molecular similarity using Chemdb tool, *Indones. J. Chem.*, 12 (3), 217–222.

[23] Saputra, A., Wijaya, K., Armunanto, R., Tania, L., and Tahir, I., 2017, Determination of effective functional monomer and solvent for R(+)-cathinone imprinted polymer using density functional theory and molecular dynamics simulation approaches, *Indones. J. Chem.*, 17 (3), 516–522.

[24] Yin, X., Liu, Q., Jiang, Y., and Luo, Y., 2011, Development of andrographolide molecularly imprinted polymer for solid-phase extraction, *Spectrochim. Acta, Part A*, 79 (1), 191–196.

[25] Tahir, I., Wijaya, K., Islam, S., and Ahmad, M.N., 2014, Computer aided design of molecular imprinted polymer for selective recognition of capsaicin, *Indones. J. Chem.*, 14 (1), 85–93.

[26] Liu, W., Qin, L., Yang, Y., Liu, X., and Xu, B., 2014, Synthesis and characterization of dibenzothiophene imprinted polymers on the surface of iniferter-modified carbon microspheres, *Mater. Chem. Phys.*, 148 (3), 605-613.

[27] Saad, E.M., Madbouly, A., Ayoub, N., and El Nashar, R.M., 2015, Preparation and application of molecularly imprinted polymer for isolation of chicoric acid from *Chicorium intybus* L. medicinal plant, *Anal. Chim. Acta*, 877, 80–9.

[28] Pardeshi, S., Patrikar, R., Dhodapkar, R., and Kumar, A., 2012, Validation of computational approach to study monomer selectivity toward the template gallic acid for rational molecularly imprinted polymer design, *J. Mol. Model.*, 18 (11), 4797–4810.

[29] Liang, D., Wang, Y., Li, S., Li, Y., Zhang, M., Li, Y., Tian, W., Liu, J., Tang, S., Li, B., and Jin, R., 2016, Study on dicyandiamide-imprinted polymers with computer-aided design, *Int. J. Mol. Sci.*, 17 (11), 1750.

[30] Nezhadali, A., Senobari, S., and Mojarrab, M., 2016, 1,4-Dihydroxyanthraquinone electrochemical sensor based on molecularly imprinted polymer using multi-walled carbon nanotubes and multivariate optimization method, *Talanta*, 146, 525–532.

[31] Mancin, F., 2017, *The strength of the interaction*, http://www.chimica.unipd.it/fabrizio.mancin/pubblica/Suprachem/II%20lezione%20Mancin.pdf, 1–32.

[32] Khan, M.S., Wate, P.S., and Krupadam, R. J., 2012, Combinatorial screening of polymer precursors for preparation of benzo-pyrene imprinted polymer: An ab initio computational approach, *J. Mol. Model.*, 18 (5), 1969–1981.